Multi-Field Coupled Simulation of Aqueous Humor in Rabbit Eye

***H.F. Song, L. Li, W.J. Wang and †Z.C. Liu**

School of Biomedical Engineering, Capital Medical University, China
Beijing Key Laboratory of Fundamental Research on Biomechanics in Clinical Application, Capital Medical University, Beijing, China

*Presenting author: songhf@ccmu.edu.cn
†Corresponding author: zcliu@ccmu.edu.cn

Abstract

Understanding the variation of the pressure difference between Anterior Chamber (AC) and Posterior Chamber (PC), as well as the state of aqueous flow, is the focus problem to know more about the progression and blinding mechanism of glaucoma. Aqueous humor plays an important role in intraocular pressure (IOP) and the increased IOP is one of the major risk factors for the primary angle closure glaucoma. Many studies did not consider the physiological variation of the Pressure Difference between PC and AC (PDPA), and the multi-field coupling effects. The aim of the present study is to investigate the aqueous humor flow based on the coupling effects of fluid-solid-heat by means of numerical simulation method.

Two models were constructed based on eye rabbit tissue sections. Model A is for multi-field coupling and Model B is for fluid-solid interaction under condition of normal IOP. ADINA (ADINA Inc.，USA) software was applied to mimic the aqueous humor flow and analyze the distribution of temperature, velocity, pressure and stress.

The contour of temperature demonstrates multiple peaks with larger value near the pupil. There is a temperature difference in the anterior segments, which plays an important role in the aqueous humor flow and affects the flow pattern and pressure distribution. The parameters demonstrate larger value when considering the temperature.

Considering the low temperature of 33^{o}C on the surface of cornea is of significance to exhibit the temperature distribution, flow pattern and pressure distribution of the aqueous humor flow. It is necessary to perform multi-field coupling simulation based on realistic PDPA measurement when studying the aqueous humor flow in eyes.

Keywords: Glaucoma; Fluid-Structure Interaction; Numerical Simulation; Aqueous Humor Flow; Ocular biomechanics

Introduction

Aqueous humor is developed in the Posterior Chamber (PC) at the ciliary body, then flows into the Anterior Chamber (AC) through the pupil, and is finally absorbed through trabecular meshwork at the angle of AC. Under steady flow condition, the ciliary body generates a steady aqueous flow rate of 2.5 μl/min[1].This flow process plays an important role in intraocular pressure (IOP) and the increased IOP is one of the major risk factors for the primary angle closure glaucoma. While the resistance of aqueous flow through the iris-lens channels increases, the Pressure Difference between PC and AC (PDPA) increases. Too high IOP will vary the aqueous humor flow patterns, the pressure distributions in the flow field and the deformations and stress distributions of it is and cornea. PDPA is the important force to maintain aqueous humor flow. Therefore, understanding the variation of PDPA, as well as the

state of aqueous flow, is the focus problem to know more about the progression and blinding mechanism of glaucoma.

The geometry dimensions of anterior segment are very small so that it is very difficult to measure its interior flow patterns via in vivo experiments. With the development of computer technology and finite element analysis, numerical simulation can be applied to mimic the flow field in the small domain of eyes.

As early as 1986, Ethier[2] calculated the flow impedance when aqueous humor flows out from juxtacanalicular. In 1988, Scott[3] performed numerical simulation of the aqueous humor flows in AC according to the temperature difference in AC. Based on a simplified 2D AC model according to the anatomical structure of eye. Canning[4] mimicked the aqueous humor flows in AC. In 2006 for the first time, Kumar [5] considered the porous property of trabecular meshwork, and constructed a simplified symmetric 3D AC model for aqueous humor flow of rabbit eye. Then, the IOP and aqueous humor flow were compared for different situations of temperature difference and pupil size. With regard to the pulsatile flow of aqueous humor from PC to AC, Abdulrazik [6] built a model to investigate the high risk factors of pupil impedance, and found the fluid dynamics difference between pulsatile flow and steady flow. Based on the establishment of a 2D model of aqueous humor flow in human AC, Ooi[7] studied the influence of aqueous humor flow on the distribution of intraocular temperature. However, this work lacks the support of experimental data, and the model was also an idealized simple model. Based on a 3D finite element model, Chai [8] mimicked influence of laser treatment on the aqueous flow and IOP, and the results might provide guidance for the treatment of decreasing IOP. A 3D symmetric model of human eye based on histological sections was built by Villamarina[9] in 2012, which considered the permeability of trabecular mesh and the temperature difference in AC, and then the flow pattern was simulated. The limitations of this work include no Fluid-Solid Interaction (FSI) was considered, the applied data was from hypothesis, and the reliability was discounted.

Although there are so many studies about aqueous humor flow, most of them are greatly simplified without considering the physiological variation of PDPA, and the coupling effects of fluid-solid-heat are rarely implemented.

The aim of the present study is to investigate the aqueous humor flow based on the coupling effects of fluid-solid-heat by means of numerical simulation method. Based on 24h continuous in vivo test of PDPA for normal IOP rabbit eyes, 3D rabbit eye models were reconstructed based on eye tissue sections, and finite element models for multi-field coupling analyses were established so as to mimic and analyze the variation rules of aqueous humor flow.

Methods

Geometry model construction of rabbit ocular segment

Histological slices of rabbit eye with HE dyeing (Figure 1) were applied to reconstruct the 3D geometry of ocular segment so as to obtain a more realistic model. Lens was not included in the slices. Thus, the lens was designed according to its realistic dimension when reconstructing the 3D model. The gap between the lens and iris at the pupil edge is H=10 μm for normal chamber angle. Model for normal rabbit eye was established according the anatomical characteristics of eye ball and the clinical characteristics of primary angle closure glaucoma (Figure 2).

Two models were constructed based on eye rabbit tissue sections. Model A is for multi-field coupling and Model B is for fluid-solid interaction.

Figure 1 Histological sections of rabbit eye

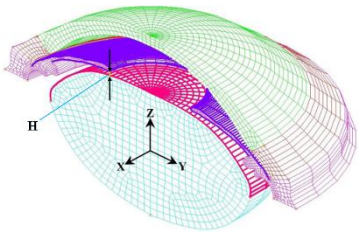

Figure 2 Reconstructed geometry model of rabbit eye

Model assumptions and parameters

Iris, cornea and lens are all of linear elastic property. The aqueous humor is incompressable laminar viscous Newtonian fluid. The upper and lower surfaces of iris and the inner suface of cornea are contacted with aqueous humor, and they are the interface of fluid-solid interaction where the no-slip condition is satisfied.

The temperature at the inner surface of cornea is 33 ^{o}C, and elsewhere 37 ^{o}C [10, 11]. The structure of trabecular meshwork at the chamber angle is porous with the porosity of α=0.5 and permeability of κ=1e^{-6} mm/s[5]. The rabbit eyes are in laying position.

Figure 3 shows the experimental data of PDPA which are the pressure boundary conditions for numerical simulation.

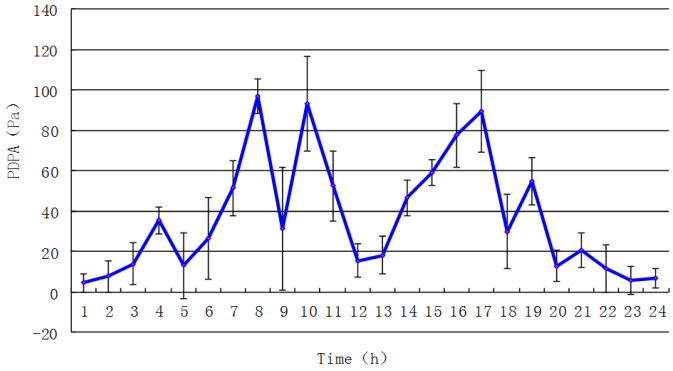

Figure 3 Experimental data of PDPA in rabbit eyes under normal IOP

The displacement of lens at y-z plane in x direction is 0 (Figure 4); The displacements at x-y plane in x, y, z directions are all 0; The displacement of trabecular meshwork at y-z plane in x direction is 0, and elsewhere are free; The displacement of cornea at y-z plane in x direction is 0, and elsewhere are free.

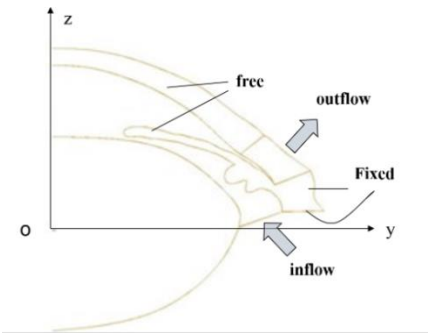

Figure 4 Boundary conditions

Material properties

According to references [7,12,13], the material properties of each part are listed in Table 1.

Table 1 Material properties

Parameter	E (kPa)	υ	c_p J(kg.K)	K (W/m.K)	ρ (kg/m^3)	μ (kg/ms)	β (1/K)
Cornea	1.19	0.49	3180	1.0042	-	-	-
Iris	6.1	0.45	4178	0.58	-	-	-
Lens	10^5	0.3	3000	0.4	-	-	-
Aqueous humor	-	-	4182	0.6	10^3	10^{-3}	$3*10^{-4}$

Note: E - Young's modulus, υ - Poison's ratio, c_p - Specific Heat Capacity, κ - coefficient of heat conductivity, ρ - density, μ - viscosity, β - coefficient of cubic expansion.

ADINA (ADINA Inc., USA) software was applied to mimic the aqueous humor flow under the multi-field coupling of fluid-solid-heat.
Five typical nodes in the model (N1~N5 in Figure 5) were selected to show the variation of flow velocity with time.

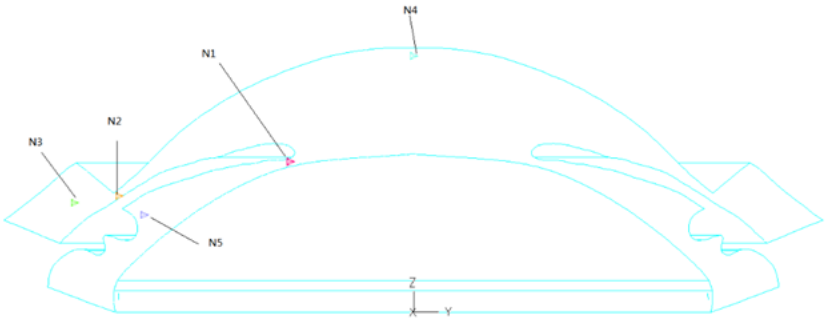

Figure 5 Nodes N1 to N5

Results

Figure 6 shows the distribution of temperature in Model A. The temperature distribution varies with time. The temperature is symmetric and decreases smoothly from iris to cornea. The contour of temperature demonstrates multiple peaks with larger value near the pupil. Temperature distribution at 8:00 AM (t=28800 s) corresponds to the moment with the largest PDPA.
Figure 7 and Figure 8 show the velocity distribution of Model A and Model B respectively. The velocity distribution is symmetric and there is a vortex in the left and right side respectively. The maximum velocity appears at the gap between the iris and pupil. The flow patterns in both models are similar while the velocity magnitude in model A is larger than that in model B.

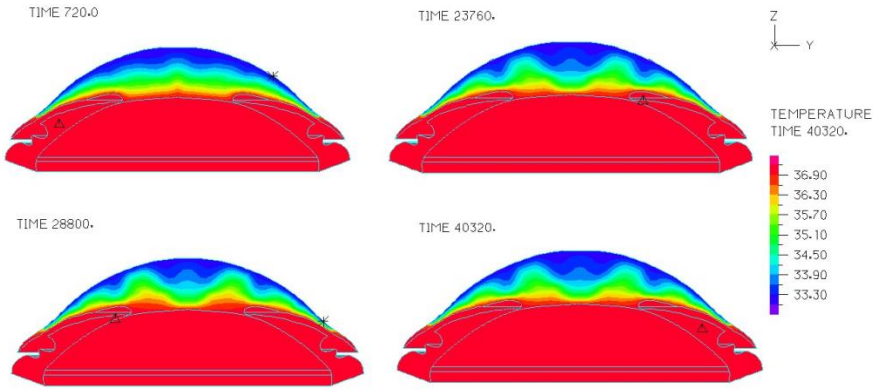

Figure 6 Distribution of temperature in model A

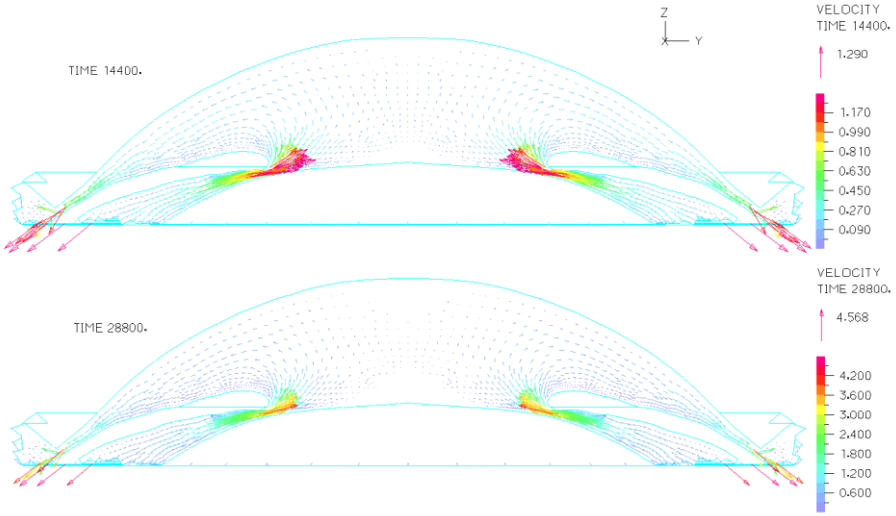

Figure 7 Velocity vector in Model A

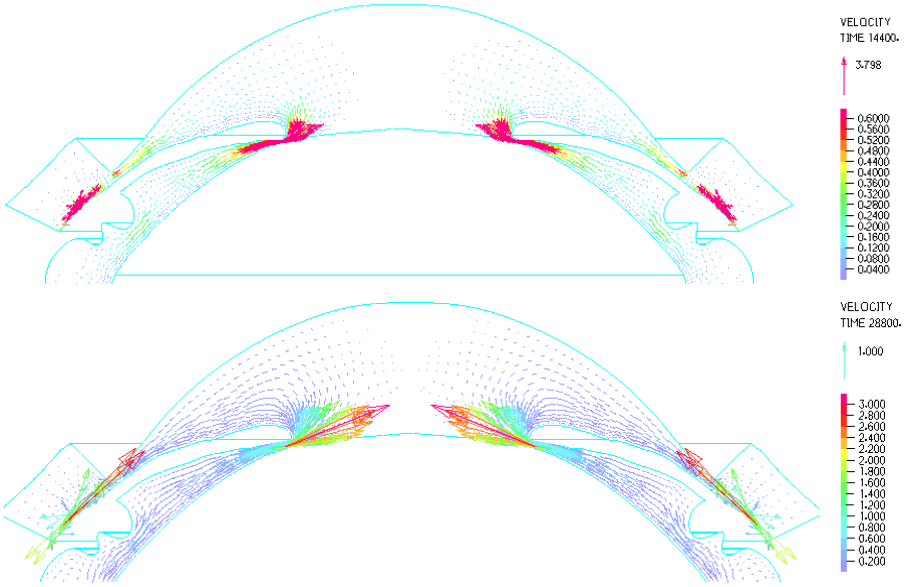

Figure 8 Velocity vector in Model B

Figure 9 shows the variation of velocities at the typical nodes in Model A. The variation rule of velocity is in agreement with that of PDPA, but the variation magnitudes are a little different. The maximum magnitudes are at N1 and N2 and that at N4 is largely constant. That is, the maximum variation of velocity locates at the gap between the iris and pupil and also at the chamber angle, while the velocity at the center of cornea rarely changes. The velocity at the gap between iris and pupil can reach 3.5 mm/s when the pressure difference is at the peak value, and the velocity at the center of cornea is nearly 0 which indicates that there is a stagnant point. The variation of velocities at the typical nodes in Model B is similar to that in Model A. Only the velocity at the AC is somewhat different. The velocity at N4 in Model A is 5.5e-3 mm/s while that in Model B is 1.49e-3 mm/s.

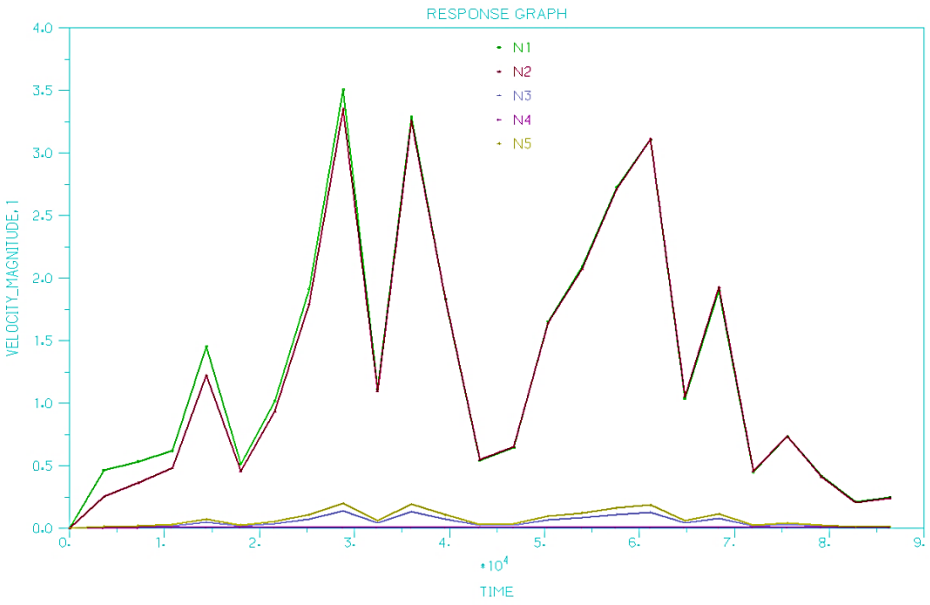

Figure 9 Variations of node velocity in Model A.

Figure 10 and Figure 11 show the contours of node pressure in Model A and Model B respectively. Pressure difference decreases gradually from PC to the cornea surface of AC. The pressure distributions in both models are similar while the pressure magnitude in model A is larger than that in model B.

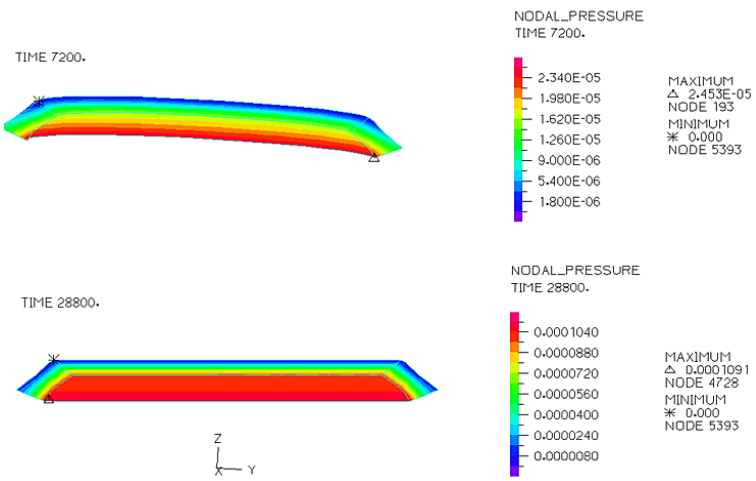

Figure 10 Contour of node pressure in Model A

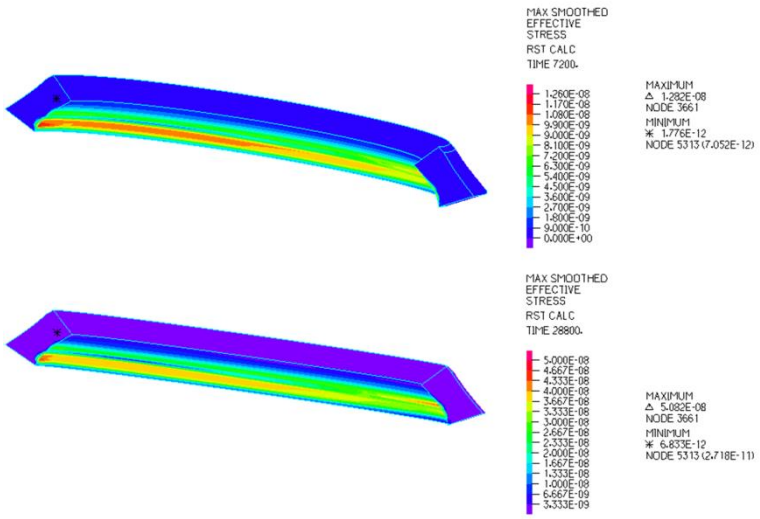

Figure 11 Contour of node pressure in Model B

Generally speaking, the parameters demonstrate larger value when considering the temperature, which indicates that the intraocular temperature plays significant rule in the aqueous humor flow, and it can influence the velocity, pressure and iris deformation.

Discussion

The distributions of temperature, velocity and pressure were investigated in this paper by means of numerical simulation. Multi-field coupling effect, which may influence the distributions of flow pattern, pressure and temperature, were considered in this study.

Results of temperature distribution in the present study are in accordance with those of Kumar[5], while quite different from those of Ooi E[7] who employed a 2D model where the geometry and boundary conditions are different.

The cornea is exposed to the air, and then some factors, such as the evaporation of tears, etc. can make the temperature of cornea outer surface equal to that of the surrounding environment, while the temperature of cornea inner surface is between 32-34^{o}C and the temperature of iris surface is the same as the body temperature of 37^{o}C. Thus, there is a temperature difference in the anterior segments, which plays an important role in the aqueous humor flow and affects the flow pattern and distribution.

The temperature difference in the AC induced buoyancy force drives the aqueous humor to flow through the iris and the cornea, then two symmetric vertices develop in the AC. This phenomenon is similar to the 2D model flow pattern in references[5,7]. The reversed flow pattern with the pressure in AC larger than that in PC can be confirmed by reference[14].

Conclusions

Considering the low temperature of 33^{o}C on the surface of cornea is of significance to exhibit the temperature distribution, flow pattern and pressure distribution of the aqueous humor flow. It is necessary to perform multi-field coupling simulation based on realistic PDPA measurement when studying the aqueous humor flow in eyes. The present work may provide reference value for understanding the flow patterns of aqueous humor flow in rabbit eye, and can help to investigate the mechanism of the development and blinding for primary angle closure glaucoma.

Acknowledgement: This work was supported by Beijing Natural Science Foundation (7152022) and National Natural Science Foundation of China (10802053).

References

[1] Mclaren, J.W., Trocme, S. D., Relf, S., and Brubaker R. F. (1990) Rate of flow of aqueous humor determined from measurements of aqueous flare. Invest. Opthalmol. *Vis. Sci*. **31**, 339-346.
[2] Ethier, C.R., Kamm, R.D., Palaszewski, B.A., Johnson, M.C., and Richardson, T.M. (1986) Calculations of flow resistance in the juxtacanalicular meshwork. *Invest Ophthalmol Vis Sci.***27**,1741-1750.
[3] Scott, J.A. (1988) A finite element model of heat transport in the human eye. *Phys Med Biol.* **33**, 227 -241.
[4] Canning, C.R, Greaney, M.J., Dewynne, J.N., and Fitt, A.D. (2002) Fluid flow in the anterior chamber of a human eye. *IMA J Math Appl Med Biol.***19**,31-60.
[5] Kumar, S., Acharya, S., Beuerman, R., and Palkama, A. (2006) Numerical solution of ocular fluid dynamics in a rabbit eye: parametric effects. *Ann Biomed Eng.* **34**,530-544.
[6] Abdulrazik, M. (2007) Model of pulsatile-flow of aqueous humor through the iris-lens canal. *Journal of glaucoma.***16**,129-136.
[7] Ooi, E., and Ng, E. (2008) Simulation of aqueous humor hydrodynamics in human eye heat transfer. *Computers in Biology and Medicine.* **38**, 252-262.
[8] Chai, D., Chaudhart, G., Mikula, E., Sun, H., and Juhasz, T. (2008) 3D finite element model of aqueous outflow to predict the effect of femtosecond laser created partial thickness drainage channels. *Lasers in surgery and medicine*, **40**,188-195.
[9] Villamarina, A., Roya, S., Hasballa, R., Vardoulis, O., Reymond, P., and Stergiopulos, N. (2012) 3D simulation of the aqueous flow in the human eye. *Med Eng Phys*, **34**,1462-1470.
[10] Mori, A., Oguchi, Y., Okusawa, Y., Ono, M., Fujishima, H., and Tsubota, K. (1997) Use of high-speed, high-resolution thermography to evaluate the tear film layer. *Am. J. Ophthalmol.***124**,729-735.
[11] Okuno, T. (1991) Thermal effect of infra-red radiation on the eye: A study based on a model. *Ann. Ocuup. Hyg.* **35**, 1-12.
[12] Yang, J., Bo, X., Qian, X., Wang, Q., Wang, J., Lu, J., Quan, H., and Liu, Z. (2010) Measuring iris elastic modulus based on holistic iris deformation experiment. *Journal of Medical Biomechanics*, **25**,182-185.
[13] Wu, L., Xie, Y., Fan, Y., Huang, X., and Luo, X. (2008) A new method used to measure corneal elastic modulus. *Journal of Sichuan University (Engineering Science edition)*, **40**, 80-85.
[14] Karickhoff, J.R. (1992) Pigmentary dispersion syndrome and pigmentary glaucoma: a new mechanism concept, a new treatment, and a new technique. *Ophthalmic Surg*. **23**, 269-277.